Short communication

Changes in electronic structure of $Li_{2-x}CuO_2$

Y. Arachi [a,*], Y. Nakata [b], K. Hinoshita [a], T. Setsu [a]

[a] Department of Chemistry, Materials Engineering, Kansai University, Suita, Osaka 564-8680, Japan
[b] Department of Science and Engineering, Iwaki Meisei University, Iwaki, Fukushima 970-8551, Japan

A R T I C L E   I N F O

A B S T R A C T

A single phase of Li_2CuO_2 was successfully prepared by solid state reaction. The crystal structure was refined by Rietveld method using a synchrotron radiation source. Electronic structures of $x = 0$ and 1 in $Li_{2-x}CuO_2$ were determined using the first principle calculation. We will discuss electrochemical properties of Li_2CuO_2 and changes in electronic structure of $Li_{2-x}CuO_2$, using both the information obtained from the calculation and that obtained experimentally. These results confirmed that Li-extraction of Li_2CuO_2 resulted in the oxidation of Cu^{2+} or O^{2-}. The cuprate-based cathode materials have the potential showing high energy density. The calculation of electronic state will play a major role in designing the materials for Li-batteries.

© 2010 Elsevier B.V. All rights reserved.

1. Introduction

New potential cathode materials with high-energy density are under extensive investigation. Li_2MnO_3-based materials with NaCl type layered structure are one of those. These materials are expected to show larger capacity by 0.5 molar or more of Li removing. For example, $LiNi_{0.5}Mn_{0.5}O_2$ shows superior characteristics for larger capacities when compared to $LiMn_2O_4$ and for better thermal stability when compared to $LiNiO_2$. We have reported the structural change behavior for $Li_{1-x}Ni_{0.5}Mn_{0.5}O_2$ in details during charging process using XRD, ND, HR-TEM and XAFS measurements [1]. It was found that a charging reaction proceeds with an oxidation of Ni^{2+} to Ni^{3+}, but not to Ni^{4+} while maintaining oxidation state of Mn^{4+} up to $x = 0.5$. However, this material shows rechargeable capacity of 150 mAh g^{-1} corresponding to $x = 0.7$ in the voltage range of 2.5–4.3 V. Considering observation of O K-edge absorption spectra during charging process, we speculate the possibility of oxygen to participate in charging process at high voltage. O ions are responsible for charge compensation during the charge–discharge as in $Li_{1-y}[Li_{0.15}Ni_{0.275-x}Mg_xMn_{0.575}]O_2$ ($x = 0$ and 0.04) [2]. The first principle calculation and XANES spectra support our expectation, the possibility of oxidation of O^{2-}. The calculation of electronic state will support to explain the charging–discharging mechanism.

In order to confirm for oxygen to participate in Li-extracting we focus on Li–Cu–O ternary oxides as a cathode material. There are several lithium cupper oxides, such as Li_2CuO_2, $LiCuO_2$, $Li_3Cu_2O_4$, and so on [3–6]. The common structure of these materials has the square planner CuO_4 with the oxygen atoms at the corners and the copper atom in the center as shown in Fig. 1. The CuO_4 plaquettes can share oxygen atoms with their nearest-neighbor plaquettes and leads to build chains or planes in the structure. This character is closely related to appearance of high-T_c superconductivity. Cuprate compounds have a fascinated character because of its abundant resources and the less toxicity. Additionally, higher cell potential can be expected in view of its electronic structure composed of trivalent Cu and O. We have begun with Li_2CuO_2 because it has large amount of Li per unit formula. The electrochemical property was reported by Arai et al. [7]. A rechargeable capacity of 130 mAh g^{-1} was obtained with an average voltage of 2.5 V against 490 mAh g^{-1} of theoretical capacity. However, there is little information on charging–discharging mechanism focused on contribution of oxygen.

Therefore, this research is primarily directed at demonstrating an electronic structure of Li_2CuO_2 and $LiCuO_2$ with emphasizing electrons of oxygen.

2. Experimental

2.1. Synthesis and measurements

The conventional solid-state reaction was used. Starting materials were composed of chemical grade Li_2CO_3 and CuO. After mixing them properly, pellets were made by the pressing under a pressure of 5 t cm^{-2}. They were calcined at 1023 K for 24 h and sintered at
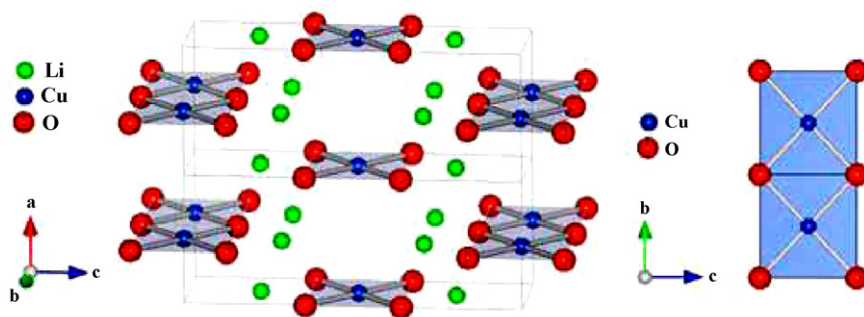

Fig. 1. Crystal structure of Li_2CuO_2 drown by VESTA [8]. Green and blue circles indicate lithium and copper, respectively. Oxygen is illustrated in large red circle. (For interpretation of the references to color in this figure legend, the reader is referred to the web version of this article.)
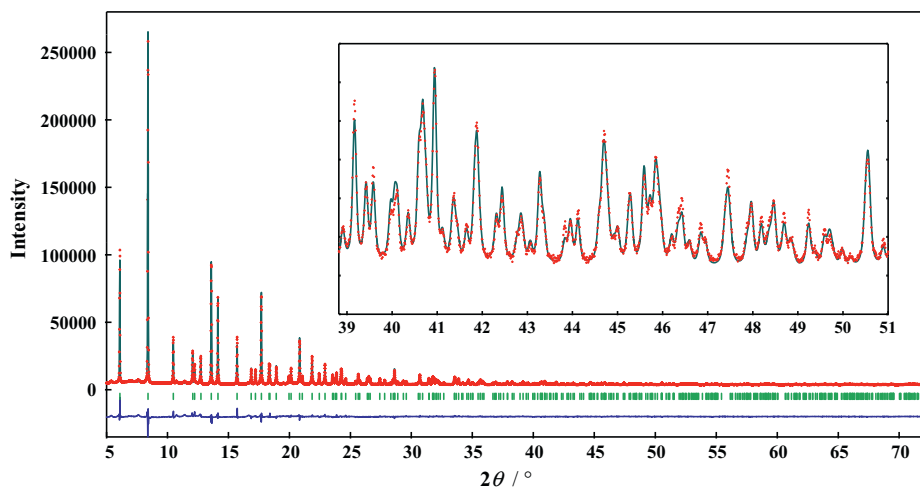

Fig. 2. Observed, calculated, and difference diffraction profiles of Li_2CuO_2 for Rietveld refinement using synchrotron X-ray diffraction data ($\lambda = 0.4991$ Å).

1073 K for 24 h in air. The obtained samples were evaluated for their crystal structure and electrochemical property. Valence state of Cu was investigated by iodometry and chemical compositions by ICP were analyzed. X-ray diffraction (XRD) measurements using a synchrotron radiation source were performed at a wavelength of $\lambda = 0.4991$ Å on BL02B2 and BL14B2 at SPring-8. The measurement used a large Debye–Scherrer camera with a radius of 286.5 mm and an imaging plate (IP) on the 2θ–θ arm as a detector. Structural refinements were carried out by Rietveld analysis using the

RIETAN-2000 computer program [9]. Electrochemical measurements were carried out galvanostatically at room temperature by HJ1001SD (HOKUTO DENKO. Ltd., Japan) apparatus using coin-type cells at a rate of 200 μA cm^{-2}. The cathode material included the sample, acetylene black and polyvinylidene fluoride (PVdF) in 60:20:20 wt% ratio. Li metal was used as a negative electrode and the electrolyte was 1 M LiClO$_4$ in propylene carbonate(PC):1,2-dimethoxycarbonate (DMC) in a 1:1 volume ratio. X-ray absorption measurements at the Cu K-, L-edges and O K-edge by total elec-
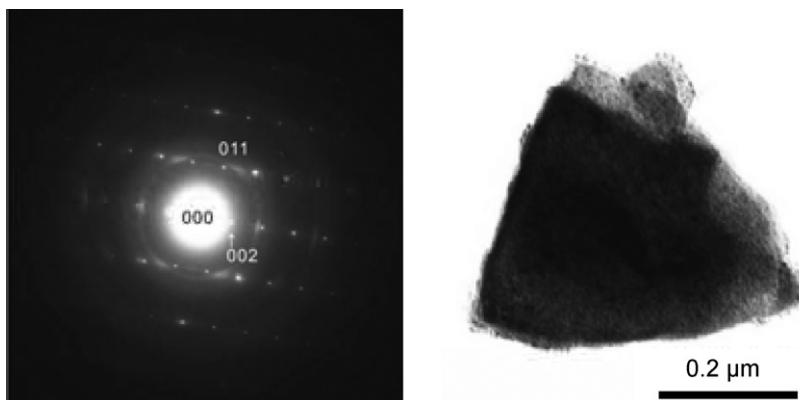

Fig. 3. Electron diffraction pattern for Li_2CuO_2 along the [1 0 0] axis.

Table 1
Summary of Rietveld refinement for Li_2CuO_2.

Site (Wyckoff letter)	x, y, z	B/Å²
Li (4j)	1/2, 0, 0.2883(4)	0.54(7)
Cu (2b)	0, 1/2, 1/2	0.227(7)
O (4i)	0, 0, 0.3588(1)	0.63(3)

$R_{wp} = 4.82$, $R_e = 1.38$, $R_I = 5.53$, $R_F = 2.62$

tron yield were performed on BL4B and BL8B1(UVSOR-II, Okazaki, Japan).

2.2. Ab initio calculation

The first principle calculations were performed using the WIEN2k program package, which is based on the full potential augmented plane wave and local orbitals (APW + lo) method within the generalized gradient approximation (GGA) [10]. The crystal structures used in the calculations are based on the crystallographic data written in [3,5]. The electronic states below the 3s and 1s states were treated as the core states for Cu and O atoms, respectively. The other states were calculated as a valence band using the APW + lo basis sets. The muffin-tin radius for Cu, O and Li were 1.85, 1.64 and 1.74 a.u. respectively. The maximum wavelength of APW, K_{max}, was determined to satisfy the condition of $R \times K_{max} = 7$, where R is the muffin-tin radius of the O atom. The warped electron density in the interstitial region was described by a finite Fourier series with maximum wave vector, G_{max}, where G_{max} satisfies 12. The maximum angular momentum l for partial spherical waves inside atomic spheres was 10. A mesh $10 \times 10 \times 10$ over the irreducible Brillouin zone was used.

3. Results and discussion

3.1. Preparation of Li_2CuO_2

XRD patterns confirmed that the obtained sample is composed of a pure single phase without any impurities such as CuO. Heat treatment to depress for Li_2O to evaporate during sintering was carried out to obtain the controlled composition. Fig. 2 shows the result of Rietveld refinement of Li_2CuO_2 and the result is summarized in Table 1. Refinement yields a good fitting by using the structure model, S.G. Immm and shows a good agreement with previous report [3]. The refined lattice parameters for orthorhombic was $a = 3.65933(3)$ Å, $b = 2.86186(3)$ Å and $c = 9.38800(10)$ Å. Chemical analysis showed that average valence state of Cu was 1.97 by iodometry and ICP analysis and chemical composition was nearly stoichiometric $Li_{2.02}Cu_{1.00}O_{2.00}$. Its magnetic property of the sample showed an anti-ferromagnetic behavior with Néel temperature, $T_N = 10$ K, which was consistent with that written in [3]. In order to observe the microstructure, electron microscopy observation was performed using TEM as shown in Fig. 3. No superstructure related to lithium-ordering was observed.

3.2. Electrochemical performance

Fig. 4 shows the results of the first and second cycle of Li_2CuO_2 using a coin type cell. In charging curve, a capacity of 490 mAh g⁻¹ was obtained, accompanied by the two noticeable plateaus at around 3.3 and 4.1 V. This behavior agreed closely with those of described in [7,11,12]. The capacity corresponds to nearly the oxidation of 2 electrons. This result allows us to discuss whether copper in divalent or oxygen of $Li_{2-x}CuO_2$ would participate in charging reaction. However, a large irreversible capacity was obtained between charge and discharge in the first cycle. The irre-
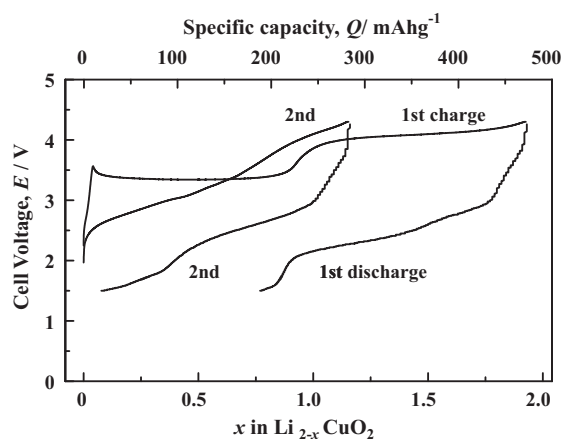
Fig. 4. Charging and discharge curves for the Li/Li_2CuO_2 cell measured with a current density of 0.20 mA cm⁻² and cut-off voltages of 1.5 and 4.3 V.

versible capacity was due to some irreversible reactions such as decomposition of electrolyte.

3.3. Electronic structure

XRD pattern for electrochemically prepared $LiCuO_2$ showed that the structure contained infinite chains of edge-sharing planner and square CuO_4 units, which was similar to those shown in Fig. 1. However, the phase was not composed of a single, but mixed one with CuO phase. Fig. 5 shows the results of density of state for $x = 0$ and 1 in $Li_{2-x}CuO_2$ by use of a first principle calculation. The number
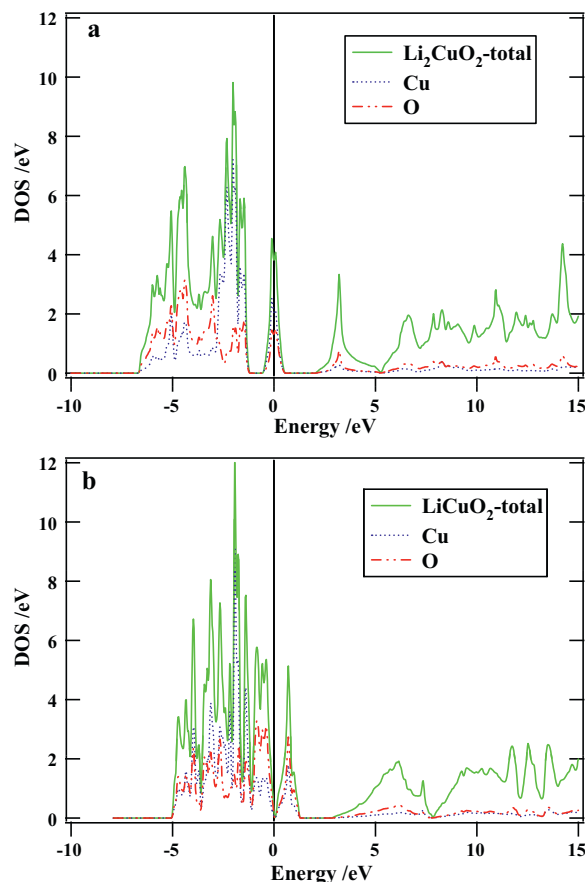
Fig. 5. Total and partial DOS of (a) $x = 0$ and (b) $x = 1$ in $Li_{2-x}CuO_2$ with the Fermi level at zero energy.

Table 2
The number of electrons for each atom in Li_2CuO_2 and Li_2CuO_2, and differences between them.

Atom	Li_2CuO_2	Li_2CuO_2	Difference
Li	2.21	2.051	0.16
Cu	26.93	26.84	0.089
O	14.55	14.16	0.194
Interstitial	5.1	4.948	0.152
Total	51	48	$=3(1 \times Li)$

of valence electron was decreased by Li-extracting and the Fermi energy shifted to a lower energy. The local density of states corresponding to $Cu3d$ and $O2p$ are located in almost same energy. In particular, these indicate a significant difference between Li_2CuO_2 and $LiCuO_2$ in a valence band state distribution of oxygen. The electronic structure of Li_2CuO_2 is comparable with that presented in [13]. The change in the number of electrons for each atom and difference between Li_2CuO_2 and $LiCuO_2$ are summarized in Table 2.

It is clearly that electrons of oxygen are reduced between them. A considerable electron loss of oxygen was occurred by Li-extraction. In order to validate the calculated electronic structure, the average cell voltages for $Li_{2-x}CuO_2$ were derived using the Nernst relationship according to the method described in [14].

$$\Delta E = E(Li_2CuO_2) - [E(LiCuO_2) + E(Li)] \tag{1}$$

$$\Delta E = 2 \times E(LiCuO_2) - [2 \times E(Li_{0.5}CuO_2) + E(L_i)] \tag{2}$$

The average voltages from (1) and (2) obtained were 0.187 Ry e^{-1} = 2.54 V and 0.355 Ry e^{-1} = 4.82 V, respectively. These calculations resemble a trend in measured charge curve as a function of lithium content.

4. Summary

A single phase of Li_2CuO_2 was successfully prepared by solid state reaction. Electronic structures of Li_2CuO_2 and $LiCuO_2$ were determined using the first principle calculation. The information obtained from the calculation was compared with that obtained experimentally. These results confirmed that Li-extraction of Li_2CuO_2 resulted in the oxidation of Cu^{2+} or O^{2-}. The cuprate-based cathode materials have the potential showing high energy density. The calculation of electronic state will play a major role in designing the materials for Li-batteries.

References

[1] Y. Arachi, H. Kobayashi, S. Emura, Y. Nakata, M. Tanaka, T. Asai, H. Sakaebe, K. Tatsumi, H. Kageyama, Solid State Ionics 176 (2005) 895–903.
[2] Y.K. Sun, M.G. Kim, S.-H. Kang, K. Amine, J. Mater. Chem. 13 (2003) 319–322.
[3] F. Sapina, J. Rodriguez-Cavajal, M.J. Sanchis, R. Ibanez, A. Beltran, D. Beltran, Solid State Commun. 74 (1990) 779–784.
[4] M.T. Weller, D.R. Lines, D.B. Currie, J. Chem. Soc. Dalton Trans. (1991) 3137.
[5] K. Imai, M. Koike, H. Takei, H. Sawa, D. Shiomi, K. Nozawa, M. Kinoshita, J. Phys. Soc. Jpn. 61 (1992) 1819.
[6] R. Berger, P. Önnerund, Y. Laligant, A.L. Bail, J. Alloys Compd. 190 (1994) 295–299.
[7] H. Arai, et al., Solid State Ionics 106 (1998) 45–53.
[8] K. Momma, F. Izumi, J. Appl. Crystallogr. 41 (2008) 653–658.
[9] F. Izumi, T. Ikeda, Mater. Sci. Forum 321–324 (2000) 198–203.
[10] P. Blaha, K. Schwarz, G.K.H. Madsen, D. Kvasnicka, J. Luitz, in: K. Schwarz (Ed.), WIEN2k, An Augmented Plane Wave plus Local Orbitals Program for Calculating Crystal Properties, Techn. Univ. Wien, Austria, 2001, ISBN 3-9501031-1-2.
[11] A.S. Prakash, D. Larcher, M. Morcrette, M.S. Hegde, J.-B. Leriche, C. Masquelier, Chem. Mater. 17 (2005) 4406–4415.
[12] N. Imanishi, K. Shizuka, T. Ikenishi, T. Matsumura, A. Hirano, Y. Takeda, Solid State Ionics 177 (2006) 1341–1346.
[13] H. Rosner, R. Hayn, S.-L. Drechsler, Physica B 259–261 (1999) 1001–1002.
[14] M. Saiful Islam, R.A. Davies, J.D. Gale, Chem. Mater. 15 (2003) 4280–4286.